# Effect of Particle Size Distribution on Monotonic Shear Strength and Stress-Dilatancy of Coarse-Grained Soils

Mandeep Singh Basson, S.M.ASCE<sup>1</sup>; Alejandro Martinez, Ph.D., A.M.ASCE<sup>2</sup>; and Jason T. DeJong, Ph.D., F.ASCE<sup>3</sup>

<sup>1</sup>Dept. of Civil and Environmental Engineering, Univ. of California, Davis, CA.

Email: mbasson@ucdavis.edu

<sup>2</sup>Dept. of Civil and Environmental Engineering, Univ. of California, Davis, CA.

Email: amart@ucdavis.edu

<sup>3</sup>Dept. of Civil and Environmental Engineering, Univ. of California, Davis, CA.

Email: jdejong@ucdavis.edu

#### **ABSTRACT**

Natural soil deposits can consist of particles with a wide range of sizes. In current practice, the assessment of shear strength and stress-dilatancy behavior of coarse-grained soils is based on methods developed for poorly graded sands, without explicit consideration for differences in gradation. This paper investigates the influence of the range of particle sizes on the monotonic shear strength and the stress-dilatancy response of poorly- to well-graded soils. Using the 3D discrete element method (DEM), the applicability of commonly used sand-based stress-dilatancy frameworks is assessed for a range of gradations. This DEM investigation employs clumps of spheres to accurately simulate the particle shapes on specimens with coefficients of uniformity (C<sub>U</sub>) varying between 1.9 and 6.9. These specimens were subjected to isotropically consolidated drained triaxial compression at various relative densities and confining stresses with the objective of isolating the effects of particle size distribution from those of particle shape. The peak and critical state shear strengths and the dilatancy responses of the specimens with different gradations are evaluated. For the same state parameter, the results indicate an increase in the shear strength and rate of dilation as the range of particle sizes increases. However, the critical state line shifts downward, and its slope decreases as C<sub>U</sub> is increased. The DEM results are compared to Bolton's stress-dilatancy relationship to highlight the inadequacies of using clean sand-based frameworks in capturing the behavior of well-graded soils.

### INTRODUCTION

The mechanical behavior of sandy and gravelly soils is typically governed by a variety of factors, including mineralogy, particle size distribution, particle shape, stress history, initial state, relative density, and inherent fabric. Widely adopted stress-dilatancy theories, presented in seminal works of Rowe (1962) and Bolton (1986), are typically based on data acquired from poorly-graded sandy soils. Several variations of these relationships have been proposed to capture the various salient features of granular material behavior. However, most of these relationships are still based on experimental data obtained for poorly graded soils (Houlsby 1991, Vaid and Sasitharan 1992, Chakraborty and Salgado 2010, Harehdasht et al. 2017). Due to a paucity of data on the behavior of well-graded soils, partly due to sample size constraints in experimental testing and computational constraints in numerical simulations, sand-based engineering approaches have been adopted to predict the response of well-graded coarse-grained

soils. Overall, these prediction procedures lead to an increase in uncertainty in the response of soils supporting critical infrastructure.

Several researchers have recently investigated the variations in stress-dilatancy and volume change of well-graded gravelly soils with high C<sub>u</sub> values. Although the published results of these investigations advance our understanding of the behavior of well-graded soils, there are still knowledge gaps and limitations. Studies have shown that increasing C<sub>u</sub> reduces the maximum and minimum void ratios, changing the relative location and slope of the critical state line in the void ratio versus mean effective stress space (Youd 1973, Fragaszy et al. 1990, Li at al. 2014, Ahmed 2019). The peak shear strength and dilative volumetric response increase with an increase in C<sub>u</sub> for drained monotonic testing (Simoni and Houslby 2006, Hamidi et al. 2012, Harehdasht et al. 2017). However, greater C<sub>u</sub> soils exhibit more contractive behavior, lower undrained strengths, and higher liquefaction potential when compared at the same void ratio (Liu et al. 2014, Li et al. 2015). Contrarily, Carey et al. (2022) report higher resistance to generation and faster dissipation of pore pressures in high C<sub>u</sub> soils when the relative density (D<sub>R</sub>) is held constant. Some studies consider coarser particles to be floating in the overall soil matrix, where variation in coarse fraction has minimal impact on the overall response (Fragaszy et al. 1992). In contrast, monotonic DSS tests on angular sands have shown a decline in shearing strength as coarser particle concentration increases (Chang and Phatachang 2016). From a micromechanical standpoint, coarser particles have higher coordination numbers in the packing and can carry the most force, implying a more significant effect on the overall behavior of well-graded soils (Wood and Maeda 2008, Li et al. 2015, Kuei et al. 2020). The lack of agreement on the influence of C<sub>u</sub> on macro- and micro-scale behavior adds to the ambiguity in soil response and can lead to over-conservative designs.

In this paper, the influence of gradation on the shear strength and stress-dilatancy behavior of well-graded soils is investigated using the discrete element method (DEM). A series of monotonic drained triaxial simulations were performed on specimens with poorly- to well-graded gradations with CU ranging from 1.9 to 6.9 over a range of state parameters. DEM is used to isolate the effect of gradation from those of particle shape and remove the effect of strain localizations, inertial effects, specimen size, and particle crushing. The overall aim of the work is to: (i) describe trends in the change in shear strength, stress-dilatancy, and volume change with soil gradationand (ii) evaluate the applicability of sand-based frameworks presented in Bolton (1986) to the response of well-graded soils.

### SIMULATION METHODOLOGY

#### **Simulated Materials**

The particle shape and gradations used in this study are based on naturally occurring coarse-grained soil sourced from a marine deposit in Mauricetown, New Jersey. The sourced soil consisted of sub-angular quartz particles and was sieved into four poorly graded soils, namely 100A, 100B, 100C, and 100D, with A having the smallest median particle size (D<sub>50</sub>) and D having the largest D<sub>50</sub>. These soils were mixed in different proportions to create well-graded soil mixtures with a range of C<sub>u</sub> values while minimizing the variability due to mineralogy and particle shape. The particle size distributions from two such mixes, 25ABCD and 33ABC, were used in this study, where the name denotes the names of the poorly graded soils used in the mixture and their mass proportion. In addition, the poorly graded soil A was also used. These

soils have been extensively researched using physical (Sturm 2019, Carey et al. 2022), laboratory (Ahmed 2021, Reardon et al. 2022), and numerical (Kuei et al. 2020, Chiaradonna et al. 2022) modeling at UC Davis. The gradations of these soils was replicated in the DEM simulations. The grain sizes were upscaled by 20 times to achieve realistic computational times (Kuei et al. 2020) Figure 1(a) shows the grain size distributions of simulated materials, and Table 1 summarizes the properties of the tested gradations.

 $\mathbf{D}_{10}$  $D_{60}$  $D_{30}$  $D_{50}$  $\mathbf{C}_{\mathbf{u}}$  $\mathbf{C_c}$ Soil e<sub>max</sub>  $e_{min}$ (mm) (mm) (mm) (mm) 100A 1.95 0.85 0.94 0.62 2.1 2.6 3.4 4.1 33ABC 4.78 0.87 0.69 0.45 3.2 6.3 10.4 14.8 25ABCD 6.94 0.66 0.62 0.39 4.1 8.2 17.6 28.2

Table 1. Average properties of the simulated gradations

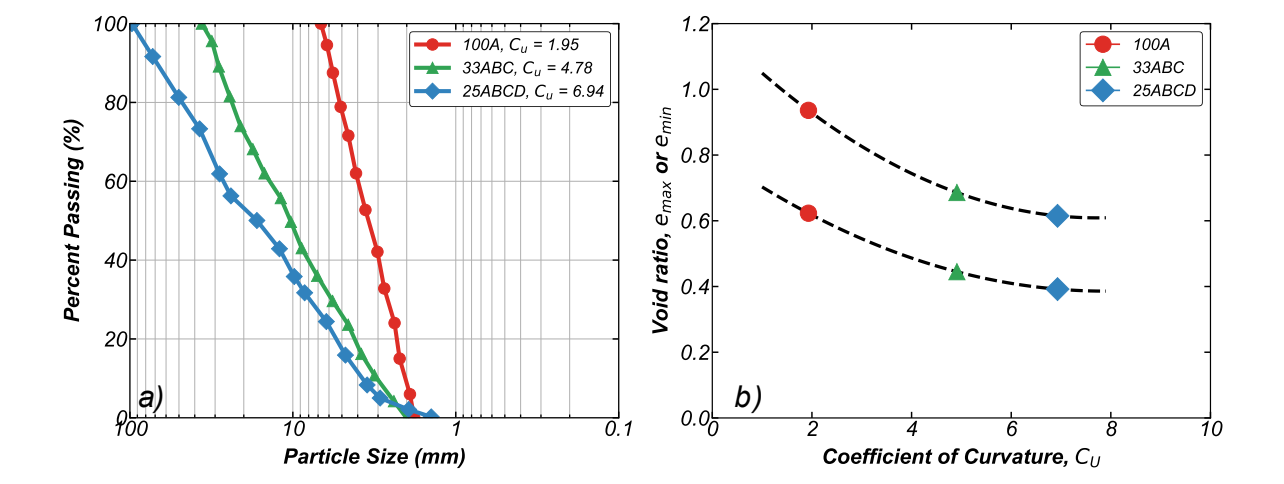


Figure 1. (a) Grain size distributions of the simulated gradations and (b) the variation of e<sub>max</sub> and e<sub>min</sub> with an increase in C<sub>u</sub>.

# Simulation methodology

The 3D DEM code YADE was used to simulate drained monotonic triaxial tests on specimens with particle gradations based on 100A, 25ABCD, and 33ABC. The particle shapes of the soils were recreated in DEM using clump templates based on the particle shapes of real sand. The real particles were scanned using a white light microscope, and the distribution of particle shape metrics, such as sphericity and SAGI (Altuhafi and Coop, 2011), were calculated using the MATLAB code developed by Zheng and Hryciw (2015). Two and three-particle clumps, shown in Figure 2, were created to fit the calculated particle shape distributions. Overall, the specimen consisted of 70% Clump 1, 10% Clump 2 and 20% Clump 3 by mass. This percentage distribution of clumps was found by conducting a parametric study and comparing the densest and the loosest state of the real and simulated sand at 100kPa of isotropic compression. The variation of e<sub>max</sub> and e<sub>min</sub> with an increasing C<sub>u</sub> from 100A to 25ABCD is presented in Figure 1(b). The plotted e<sub>max</sub> and e<sub>min</sub> were obtained by providing an inter-particle friction coefficient of

0.5 and 0.01, respectively, during the simulation. The trends of  $e_{max}$  and  $e_{min}$  for simulated gradations are consistent and in range with those previously reported in experimental testing (Youd 1973, Fragaszy 1990, Ahmed 2021).

Monotonic drained triaxial (TX) simulations were conducted on cubical specimens to characterize the stress-dilatancy and strength of the tested gradations. Periodic boundary conditions were employed on all the boundaries to avoid strain localization and ensure uniform deformational fields within the specimens (Huang et al. 2014). A uniform strain field was applied in the vertical direction to achieve drained conditions, whereas the confining stress was maintained in the horizontal direction using stress-based servo control algorithms. Around 50000 clumps (120000 particles) were simulated for 100A gradation, and 75000 clumps (~190000 particles) were simulated for 25ABCD and 33ABC gradations foreach specimen. The sample size (D<sub>specimen</sub>) was approximated based on the maximum the following two conditions: 20 times  $D_{50}$  or 5 times the largest particle diameter ( $D_{max}$ ). In this study, the  $D_{specimen}/D_{50}$  varied between 20.54 for 25ABCD and 26.11 for 100A, which are generally consistent with the recommendations in literature (O'Sullivan 2011). A linear elastic contact model with a Mohr-Coulomb plasticity without cohesion was used to simulate the interactions between the particles. The normal stiffness of the contact was based on the stiffness (k<sub>n</sub>) and D<sub>50</sub> of the particles in contact. A particle stiffness to  $D_{50}$  ( $k_p/D_{50}$ ) ratio of 2.5e8 N/m<sup>3</sup>, shear to normal stiffness ( $k_s/k_p$ ) ratio of 0.2, particle density (p) of 2650 kg/m<sup>3</sup>, and global damping of 0.05 were used in the simulations. Gravity and particle crushing were not modeled in these simulations. To prepare the specimen for TX testing, a cloud of clumped particles was isotropically compressed to a mean effective stress of 100 kPa, 400 kPa, and 800 kPa. Once prepared, the specimen was sheared under a constant shear rate and constant confinement to an axial strain of 25%. To achieve a quasi-static response, the sample preparation and shearing rate were controlled such that the inertial number was below 10<sup>-4</sup> and the unbalanced force ratio were below 10<sup>-2</sup> (da Cruz et al. 2005). The stresses and strains were tracked in a measurement cube with dimensions slightly smaller than the size of the specimen. The repeatability of the simulations was checked by rerunning specimens constructed with varying seed parameters, which influence the exact location of particles within the specimens.



Figure 2. Clump templates created to recreate the realistic particle shape.

# RESULTS AND DISCUSSION

#### **Monotonic Drained Triaxial Response**

The evolution of deviatoric stress (q) and volumetric strain (e<sub>v</sub>) with axial strain (e<sub>a</sub>) for the three gradations, 100A, 33ABC, and 25ABCD, is illustrated in Figures 3 and 4. For brevity, only

the evolutions at tests at a confining stress of 100 kPa and 400 kPa are presented. Nonetheless, the trends are similar for specimens tested at 800 kPa confining stress. The state parameter, defined as the difference between the start and critical void ratios (Been and Jefferies, 1985), is used to differentiate between the loose and dense of the critical specimens. The critical state lines used to calculate the state parameters are shown in the following section. For both confining stress levels, the specimens with positive state parameters show a contractive behavior without mobilization of a peak shear strength, typical of loose soils. In contrast, the specimens with negative state parameters shows a dilative behavior with a distinct peak deviatoric stresses accompanied by strain-softening, typical of dense soils. At strains greater than 20%, the deviatoric stress of the specimens at different initial state parameters converge to the same value and no more volume changes occur. The higher mean effective confining stress in the simulations at 400 kPa results in greater magnitudes of deviatoric stress, delays the onset of peak stress to a higher axial strain, decreases the rate of dilation and decreases the final volumetric strains for all the tested gradations. For example, 25ABCD specimen with a state parameter of -0.101 at 100 kPa reaches a peak deviatoric stress of 413 kPa at 2.98% strain with a volumetric strain of 6.7% at critical state, while the specimen with a state parameter of -0.083 at 400 kPa reaches a peak q of 1420 kPa at 4.52% axial strain with a volumetric strain 5.5% at critical state. These observations indicate that the dilative tendencies are suppressed with an increase in the confining stress.

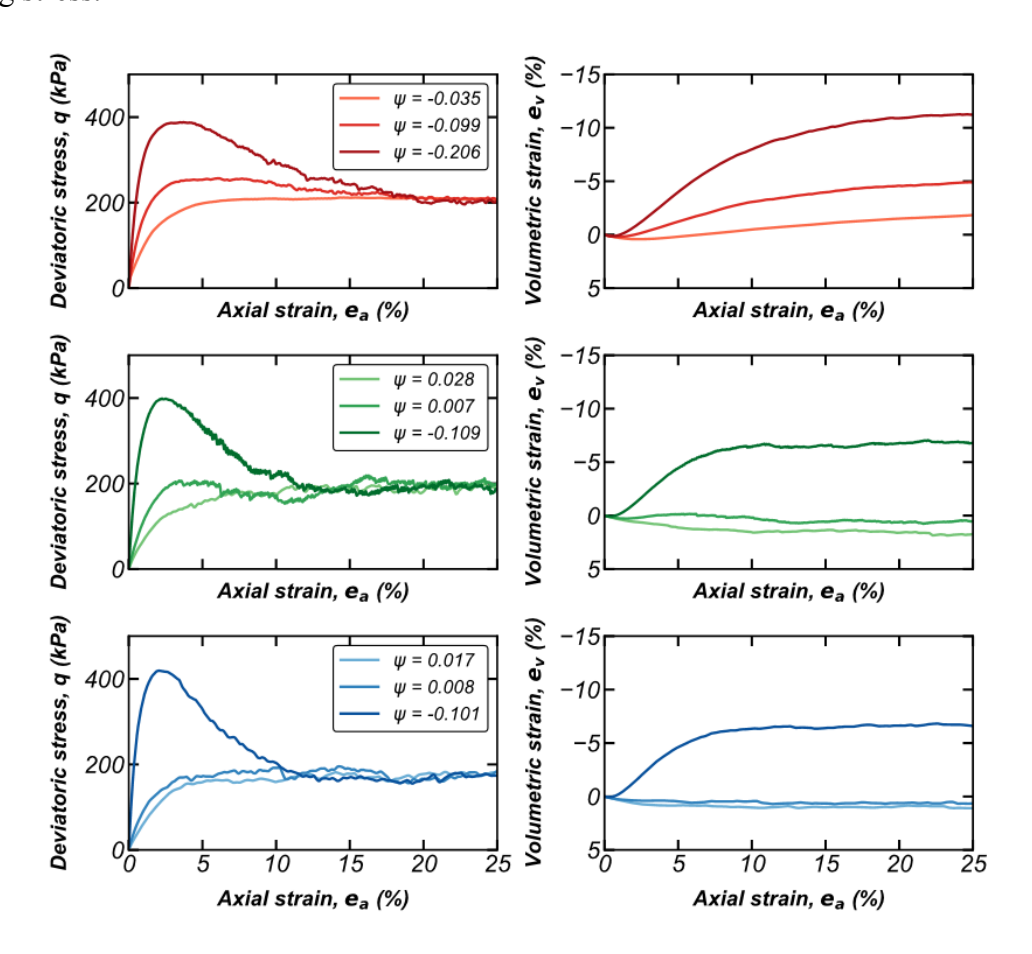


Figure 3. Monotonic drained TX results presented as deviatoric stress-strain and volumetric strain response at 100kPa.

A comparison of the stress ratio (q/p') and volumetric strains for the specimens at near-identical state parameters for the three gradations is presented in Figure 5. The 25ABCD and 33ABC gradations mobilize greater q/p' values than that mobilized by the 100A specimen (Fig. 5(a)). At the peak state, 25ABCD mobilizes the highest stress ratio, followed by 33ABD and 100A, respectively. However, 100A has the highest stress ratio at the critical state, followed by 33ABCD and 25ABCD, respectively. The volumetric strains follow a similar pattern, with 25ABCD and 33ABC showing a stronger dilative response than 100A and a higher dilation rate and final volumetric strains (Fig. 5(b)). The dilation rate and volumetric strains for 25ABCD are the greatest, followed by 33ABC and 100A, indicating that the wider gradation produces a more dilative response.

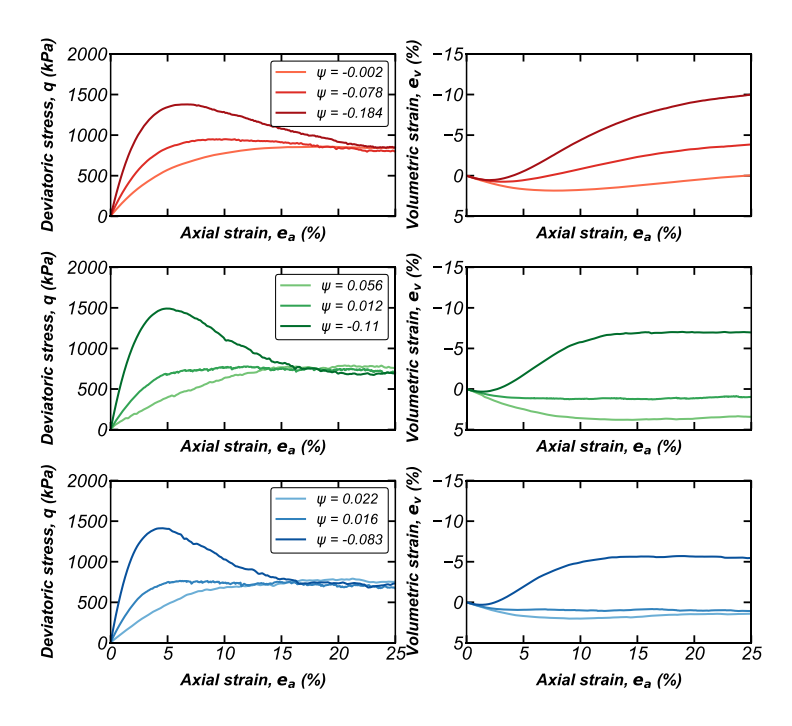


Figure 4. Monotonic drained TX results presented as deviatoric stress-strain and volumetric strain response at 400kPa.

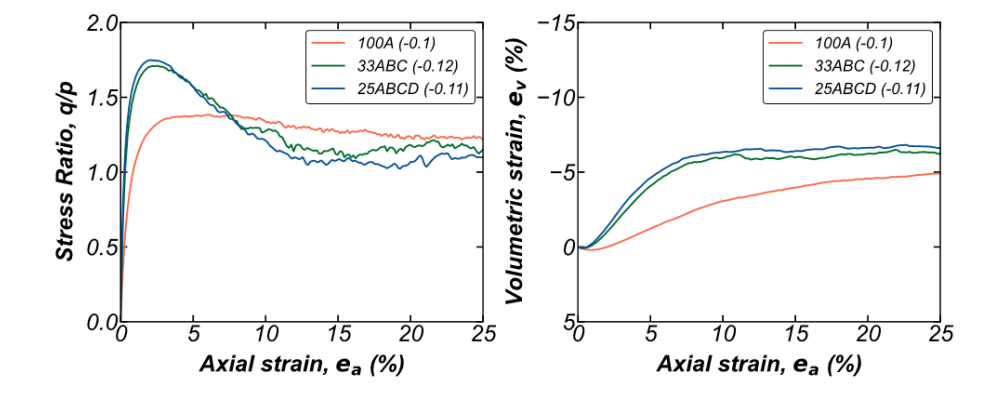


Figure 5. Comparison of (a) stress ratio, (b) volumetric strains for the tested gradations at 100 kPa.

#### **Critical State Lines**

The critical state lines (CSL) in the q-p' and the e-log(p') plane were estimated using the average of the measurements obtained for the last 1% strain for each triaxial test. The critical state lines for 100A, 33ABC, and 25ABCD based on tests at confining pressures of 100kPa, 400kPa, and 800kPa are presented in Figure 6. The critical state friction angle,  $\phi'_{cs}$ , was calculated by fitting the critical state points in the q-p' space with a straight line passing through the origin to define the slope M. The peak angle,  $\phi'_{p}$ , was calculated using the maximum q/p' mobilized in each test. A clear curvature can be observed for the CSL in the e-log(p') space, due to which the CSL was approximated using the power function as follows:

$$e_{cs} = e_{ref} - \lambda \left( p'/p_{at} \right)^{\xi} \tag{1}$$

where  $e_{ref}$  is the reference void ratio controlling the position in the CSL,  $\lambda$  controls the slope of the CSL,  $p_{at}$  is atmospheric pressure (101.325 kPa), and  $\xi$  is a material constant (Wang et al. 2002). In this study,  $\xi$  is fixed at 0.7 based on recommendations from Li and Wang (1998). The obtained critical state measurements were fitted with equation (2) using non-linear least squares by Levenberg-Marquardt's fitting procedure and plotted in Figure (6).

The fitted CSL indicate that the soil gradation affects the M,  $e_{ref}$ , and  $\lambda$  parameters. With increasing  $C_u$ , the M slope decreases from 1.21 ( $\phi'_{cs} = 30.2^{\circ}$ ) for 100A to 1.15 ( $\phi'_{cs} = 28.8^{\circ}$ ) for 33ABC and 1.13 ( $\phi'_{cs} = 28.3^{\circ}$ ) for 25ABCD. The  $\phi'_{cs}$  values are in agreement with general values for quartz sands, and the small variation in M and  $\phi'_{cs}$  with an increase in  $C_u$  agrees with results presented in the literature (e.g. Hamidi et al. 2012, Harehdasht et al. 2017, Reardon et al. 2022). The  $e_{ref}$  decreases with an increase in  $C_u$  from 0.92 for 100A to 0.59 for 25ABCD. Similarly, the  $\lambda$  decreases for an increase in  $C_u$  ranging from 0.015 for 100A to 0.006 for 25ABCD. An increase in  $C_u$  values creates a decrease in the  $e_{max}$  and  $e_{min}$  (Fig. 1(b)), affecting the location of  $e_{ref}$ . Furthermore, for high  $C_u$  soils, a significant volume of small particles filling in the voids decreases the overall compressibility of the specimen, resulting in a decrease in the  $\lambda$  parameter. Similar observations for the decrease in  $e_{ref}$  and  $\lambda$  with an increase in  $C_u$  are presented for various high  $C_u$  soils in the literature (e.g., Li et al. 2014, Althuafi and Coop 2011, Ahmed 2021).

#### **Evaluation of Stress-Dilatancy Framework**

The stress-dilatancy measurements obtained for 100A, 25ABCD, and 33ABC are presented according to Bolton's (1986) framework to test the applicability of this sand-based method over a variety of gradations. The results based on Bolton's framework are shown in Figure 7(a), which compares the mean effective stress, p', to the difference in peak and critical state friction angles  $(\phi_p^i - \phi_{cs}^i)$ . The empirical trendlines proposed by Bolton from the dataset of 17 poorly-graded sands ( $C_u < 1.9$ ) are included for relative densities of 25, 50, 75, and 100%. The 100%  $D_R$  line delineates a specimen prepared at the  $e_{min}$  void ratio, the densest possible state with a highly dilative response. The values for the poorly-graded 100A mix with highly negative state parameters (-0.206, -0.184, -0.144) are typically within the 100% density line range. However, the data for the 33ABC and 25ABCD specimens with state parameters less than -0.1 plot at locations higher than the Bolton trendline for  $D_R$ =100%. The difference between Bolton's prediction and observed response becomes greater with increasing confining stress. Furthermore, the mesurements obtained for the 25ABCD specimen exhibit the largest  $\phi_p^i$  -  $\phi_{cs}^i$  for most

confining stress, followed by 33ABC and 100A. Based on the above observations, it is reasonable to conclude that the wider 25ABCD and 33ABC gradations lead to a more dilative soil response than the 100A gradation and the poorly-graded soils reported in Bolton (1986).

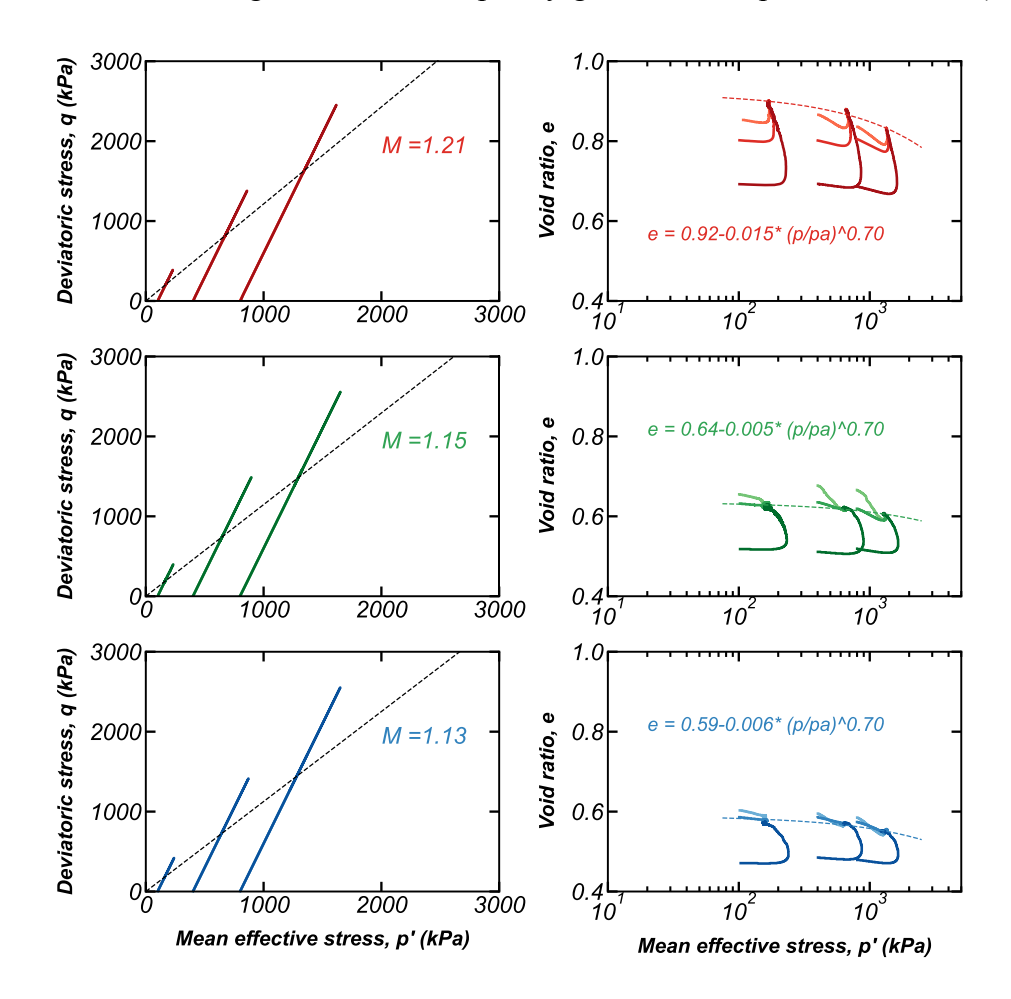


Figure 6. Critical state lines and respective fittings for the q-p' and e-log(p') spaces.

Bolton (1986) also modified Rowe's stress-dilatancy relationship, between the  $\phi'_p$  -  $\phi'_{cs}$  and maximum dialtion angle ( $\psi_{max}$ ), with a scalar correction (b) given as:

$$\phi'_{p} - \phi'_{cs} = b \cdot \psi_{max} \tag{2}$$

This correction factor (b) accounts for energy losses and provides an adjustment for the difference in the shearing mode for the direct shear and triaxial testing, with typical values for triaxial shearing ranging from 0.3 to 0.6 (Chakraborty and Salgado). Figure 7(b) presents the results for 100A, 25ABCD and 33ABC specimens with a dilative response. A best fit straight line with an intercept at origin was fitted to obtain the b parameter. The fitted results show that the parameter b is within the range of values provided in the literature, with a minimum b value of 0.301 for 100A, an intermediate value 0.377 for 33ABC, and a maximum b value of 0.415 for 25ABCD. This increase in b with C<sub>U</sub> indicates that the existing correlations may not propertly account for gradation variations for soils.

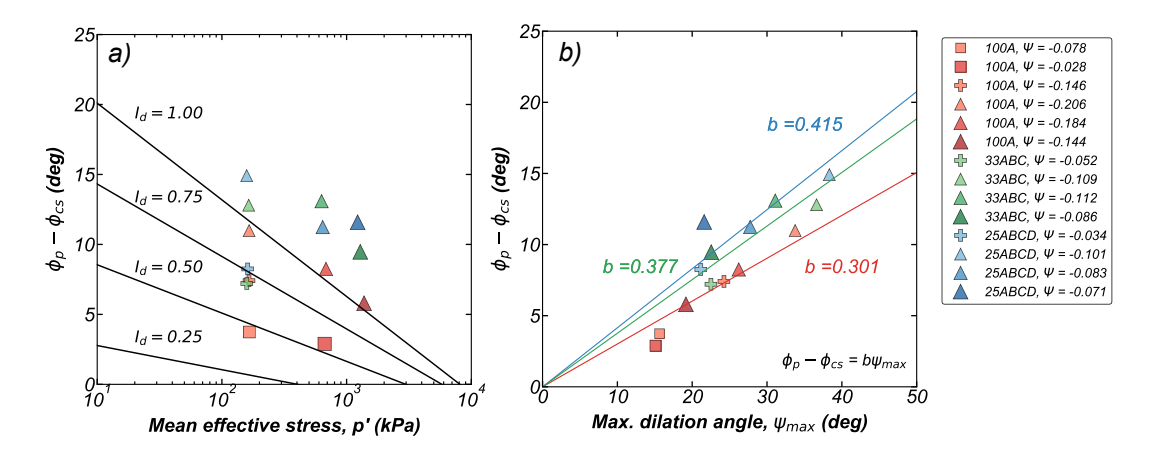


Figure 7. (a) Stress-dilatancy behavior, and (b) comparison of shearing resistance versus maximum dilatancy of monotonic drained triaxial tests as per Bolton (1986).

#### CONCLUSIONS

A series of monotonic drained triaxial 3D DEM simulations were performed on specimens of three different particle size distributions to systematically investigate the effect of widening gradation on the shear strength, volume change, and stress-dilatancy of coarse-grained soils. An attempt was made to mimic the realistic particle shape in simulations by employing clump templates in the DEM simulations. Evolutions of stresses and volume changes were presented along with estimated critical state lines in the q-p' and e-log(p') planes. Test results indicate an increase in peak shear strength, higher rate of dilations, larger volumetric strains at critical state, and a decrease in  $e_{ref}$  and  $\lambda$  parameters with widening gradation. The applicability of commonly used sand-based stress-dilatancy framework to a range of  $C_u$  levels was evaluated. Overall, while not unreasonable, the stress-dilatancy frameworks fail to account for the significantly dilative response of soils with wide gradations corresponding to  $C_U$  values of 4.9 and 6.9. The findings presented here can contribute to further the understanding of well-graded granular materials. Future studies will focus on assessing the ability of liquefaction triggering frameworks to predict the response of soils with varying gradation.

# **ACKNOWLEDGEMENTS**

Financial support for this project comes from the National Science Foundation (NSF) under Grant CMMI-1916152. Any opinions, findings, conclusions, or recommendations expressed in this paper are those of the authors and do not necessarily reflect the views of NSF. The authors would also like to acknowledge collaboration with the experimental testing team (Rachel Reardon, Francisco Humire, Sharif Ahmed), centrifuge modeling team (Trevor Carey, Nathan Love, Anna Chiaradonna), and numerical simulation team (Katerina Ziotopoulou) for their contributions to the project.

#### REFERENCES

Ahmed, S. S. (2021). Study on Particle Shape, Size and Gradation Effects on the Mechanical Behavior of Coarse-Grained Soils, PhD Thesis. University of California, Davis.

- Altuhafi, F. N., and Coop, M. R. (2011). "Changes to particle characteristics associated with the compression of sands." *Géotechnique*, 61(6), 459-471.
- Been, K., and Jefferies, M. G. (1985). "A State Parameter for Sands." *Géotechnique*. 35(2), 99-112.
- Bolton, M. D. (1986). "The strength and dilatancy of sands." Géotechnique, 36(1), 65–78.
- Carey, T. J., Chiaradonna, A., Love, N. C., Wilson, D. W., Ziotopoulou, K., Martinez, A., and DeJong, J. T. (2022). "Effect of soil gradation on embankment response during liquefaction: A centrifuge testing program." *Soil Dynamics and Earthquake Engineering* 157, p. 107221.
- Chakraborty, T., and Salgado, R. (2010). "Dilatancy and shear strength of sand at low confining pressures." *Journal of Geotechnical and Geoenvironmental Engineering*, 527–532.
- Chang, W. J., and Phantachang, T. (2016). Effects of gravel content on shear resistance of gravelly soils. *Engineering Geology*, 207, 78–90.
- Chiaradonna, A., Ziotopoulou, K., Carey, T. J., DeJong, J. T., and Boulanger, R. W. (2022). "Dynamic Behavior of Uniform Clean Sands: Evaluation of Predictive Capabilities in the Element- and the System-Level Scale." In *Geo-Congress 2022*. American Society of Civil Engineers.
- Da Cruz, F., Emam, S., Prochnow, M., Roux, J., and Chevoir, F. (2005). "Reophysics of dense granular materials: Discrete simulation of plane shear flows." *Physical Review*, 72, 021309.
- Fragaszy, R. J., Su, W., and Siddiqi, F. H. (1990). "Effects of oversize particles on the density of clean granular soils," *Geotechnical Testing Journal, GTJODJ*, 13(2), 106-114.
- Fragaszy, R. J., Su, W., Siddiqi, F. H., and Ho, C. L. (1992). "Modeling strength of sandy gravel," *Journal of Geotechnical Engineering Division*, ASCE, 118(6), 920-935.
- Hamidi, A., Azini, E., and Masoudi, B. (2012). "Impact of gradation on the shear strength-dilation behavior of well graded sand-gravel mixtures." *Scientia Iranica*, 19(3), 393–402.
- Harehdasht, S. A., Karray, M., Hussien, M. N., and Chekired, M. (2017). "Influence of particle size and gradation on the stress-dilatancy behavior of granular materials during drained triaxial compression." *International Journal of Geomechanics*, 17(9).
- Houlsby, G. T. (1991). "How the dilatancy of soils affects their behaviour." In *Proceedings of the Tenth European Conference on Soil Mech. and Foundation Engg.*, Vol. 4. pp. 1189–1202.
- Huang, X., Hanley, K. J., O'Sullivan, C., and Kwok, F. C. (2014). "Effect of sample size on the response of DEM samples with a realistic grading." *Particuology*. 15, 107-115.
- Kuei, K. C., DeJong, J. T., and Martinez, A. (2020). "Particle Size Effects on the Strength and Fabric of Granular Media." In *Geo-Congress* 2020, American Society of Civil Engineers.
- Li, X. S., and Wang, Y. (1998). Linear representation of steady-state line for sand. J *Journal of Geotechnical and Geoenviromental. Engineering* 12(1215), 1215–1217.
- Li, G., Liu, Y., Dano, C., and Hicher, P. (2014). "Grading-Dependent Behavior of Granular Materials: From Discrete to Continuous Modeling." *J. Eng. Mech.* 141(6), 04014172.
- Liu, Y., Li, G., Yin, Z., Dano, C., Hicher, P., Xia, X., and Wang, J. (2014). "Influence of grading on the undrained behavior of granular materials." *Comptes Rendus Mecanique*. 342, 85-95.
- O'Sullivan, C. (2011). *Particulate Discrete Element Modelling a Geomechanics Perspective* Spon Press, London.
- Reardon, R., Humire, F., Ahmed, S. S., Ziotopoulou, K., Martinez, A., and DeJong, J. T. (2022). "Effect of Gradation on the Strength and Stress-Dilatancy of Coarse-Grained Soils: A Comparison of Monotonic Direct Simple Shear and Triaxial Tests." In *Geo-Congress* 2022, American Society of Civil Engineers.

- Rowe, P. W. (1962). "The stress-dilatancy relation for static equilibrium of an assembly of particles in contact." *Proceedings of the Royal Society of London. Series A. Mathematical and Physical Sciences*, 269(1339), 500–527.
- Simoni, A., and Houlsby, G. T. (2006). "The direct shear strength and dilatancy of sand-gravel mixtures." *Geotechnical and Geological Engineering*, 24(3), 523–549.
- Sturm, A. P. (2019). On the liquefaction potential of gravelly soils: characterization, triggering and performance. PhD Thesis. University of California, Davis.
- Vaid, Y. P., and Sasitharan, S. (1992). "The strength and dilatancy of sand." *Canadian Geotechnical Journal*, 29(3), 522–526.
- Wang, Z.-L., Dafalias, Y. F., Li, X.-S., and Makdisi, F. I. (2002). "State pressure index for modelling sand behaviour." *Journal of Geotechnical and Geoenviromental. Engg.* 128(6), 511-519.
- Wood, D. M., and Maeda, K. (2008). "Changing grading of soil: effect on critical states". *Acta Geotechnica*. 3, 3-14.
- Youd, T. L. (1973). "Factors controlling maximum and minimum densities of sands. Evaluation of Relative Density and its Role in Geotechnical Projects Involving Cohesionless Soils." In STP 523. ASTM International. West Conshohocken, PA. pp. 98–112.
- Zheng, J., and Hryciw, R. D. (2015). "Traditional soil particle sphericity, roundness and surface roughness by computational geometry." *Geotechnique* 65(6), 494–506 (2015).